Nuclear Instruments and Methods in Physics Research A 729 (2013) 19–24

Contents lists available at ScienceDirect

Nuclear Instruments and Methods in Physics Research A

journal homepage: www.elsevier.com/locate/nima

Tunable THz radiation generation using density modulation of a relativistic electron beam

Sandeep Kumar [a,*], Dong-Eon Kim [b,c], Heung-Sik Kang [a]

[a] Pohang Accelerator Laboratory, San 31, Hyoja-dong, Pohang, Kyungbuk, Republic of Korea
[b] Department of Physics, Center for Attosecond Science and Technology (CASTECH), Pohang University of Science and Technology (POTECH), San 31, Hyoja-dong, Pohang, Kyungbuk 790-784, Republic of Korea
[c] Max Planck Center for Attosecond Science, POSTECH, San 31, Hyoja-dong, Pohang, Kyungbuk 790-784, Republic of Korea

ARTICLE INFO

Article history:
Received 25 March 2013
Received in revised form
26 June 2013
Accepted 1 July 2013
Available online 5 July 2013

Keywords:
Density modulation
Energy modulation
THz radiation
Electron beam
CEP laser

ABSTRACT

At Pohang Accelerator laboratory, at fs–THz facility, 3 THz radiation was achieved successfully using electron bunch shorter than 200 fs pulse width. To further enhance the radiation bandwidth, we use density modulation of a relativistic electron beam. In this method, a 70 MeV electron beam is first energy modulated by two optical laser-modulator and then density modulated using chicane. The density modulation at 12 THz is observed by down-converting the frequency of lasers with 800 nm and 1550 nm wavelength. The generated central frequency is found tunable for other combination of laser wavelength also. Due to proper synchronization of this THz radiation with the optical lasers; a high temporal resolution for the optical-pump THz-probe experiments can be achieved. The realization of this technique at fs–THz beamline at the PAL will enable us to make a substantial progress towards the tunable narrowband THz sources.

1. Introduction

THz generation has been an active field of research proposal for the scientist worldwide. Terahertz (THz) radiation, which is located between the infrared light and microwaves in the frequency domain, attracts much interest due to its wide applications [1–6]. However actual applications have been limited by the lack of suitable THz light source. In accelerator-based radiation sources, ultra-short electron-bunches (femtosecond or picosecond order) have been the key elements and widely used to generate ultra-intense radiation [7,8]. Coherent THz radiation using ultra-short electron bunches [9] has been investigated over past years [10–14]. For broad band THz radiation, electron bunches are compressed to picosecond level or sub-ps level and then transported for the transition radiation, diffraction radiation, synchrotron radiation, undulator radiation, etc. But the generated radiation has limited THz frequency bandwidth. It becomes very difficult to extend the radiation bandwidth over than 5 THz as it would require the electron bunch length shorter than sub-100 fs level. For a 50 MeV electron beam, the shortest bunch length is limited by nonlinear effects in the bunch compression and the space charge effects. Moreover if we compress the electron beam too much it leads to the degradation of the electron beam quality. Some application of THz radiation, for example in THz imaging, powerful narrowband THz radiation is required. To provide such kind of sources, density modulated micro-bunched electron beam repeated at THz frequency was proposed [15,16].

In one technique, a train of laser pulses is used to shine the photocathode to generate a train of electron beams repeated at THz frequency and use them for narrowband THz. Unfortunately space charge forces deteriorate the longitudinal phase distribution during acceleration process and may limit the application to the relatively low current beam. To mitigate the influence of the space charge effect, it is important to generate density modulation of electron beam when they are at relativistic energy. In this technique, typically a laser is first used to interact with the beam in a short undulator to generate energy modulation at the laser frequency; then the energy modulation is converted into density modulation after the beam passes through a dispersive chicane. As a result, the beam density is modulated at both the laser frequency and its harmonics. The density modulated beam is extensively used to drive seeded FELs to generate fully coherent radiation at high harmonic frequencies of the seed laser for current enhancement and for increasing temporal coherence [17–24].

At Pohang accelerator laboratory (PAL), at the fs–THz beamline, the radiation is expected to cover up to 3 THz ($\sim$100 cm^{-1}) frequency with the pulse width $<$200 fs using the coherent transition radiation method [25]. Time resolved THz spectroscopy is planned to study chemical and biological reaction dynamics as well as THz time domain spectroscopy (TDS). To enhance this THz

* Corresponding author. Tel.: +82 542791135.
E-mail address: skumar@postech.ac.kr (S. Kumar).

0168-9002/$ - see front matter © 2013 Elsevier B.V. All rights reserved.
http://dx.doi.org/10.1016/j.nima.2013.07.001

radiation bandwidth over 5 THz, another scheme, similar to the well known difference frequency generation (DFG) technique is under consideration. This scheme is widely used in laser community for narrowband THz radiation using relativistic electron beam as a nonlinear medium [26]. Based on DFG, higher, narrowband THz radiation was obtained through down conversion of the frequency of optical lasers by using laser modulated electron beams. The advantage of this scheme is that THz radiation will be tunable and in tight synchronization with lasers to give high temporal resolution [27]. Recently using the DFG scheme, perfectly coherent, 10 THz radiation has been shown experimentally by using laser modulated electron beam and the possibility of tunable radiation for other wavelengths has been discussed [28].

In this paper, we employ this idea at the fs–THz beamline at PAL. We consider the same electron beam parameters as of the present fs–THz beamline as this scheme can be realized by small modification at the fs–THz beamline. We use two external lasers for energy modulation of the electron beam, and two short modulators and one dispersion section for density modulation. We generate energy modulation in a relativistic electron beam before modulating the density in chicane. We present the simulation results of the density modulated electron bunch. The structure of the paper is given as follows. In Section 2, we present the schematic layout of the scheme. We use a 70 MeV electron bunch for our simulation. In Section 3, we present the simulation results obtained by using this scheme. Finally in Section 4, we present the conclusions of the results.

2. Proposed scheme at fs–THz experiment at Pohang accelerator laboratory

Fig. 1 shows the scheme for tunable broadband narrow THz radiation generation. A carrier envelope phase (CEP) laser shines the cathode of radio-frequency (RF) gun to generate the electrons. These electrons get accelerated from a zero velocity to the relativistic velocity under strong RF accelerating field. Two accelerators AC1 and AC2 as shown in Fig. 1 are used to accelerate the electron beam up to 70 MeV. Later this electron beam is modulated in energy in two different laser-modulator systems. In first modulator U1, an 800 nm laser modulates the electron beam and in second modulator U2, a laser with variable wavelength is used for the energy modulation. Further in the downstream, a dispersion section is used to make a density modulated electron beam. The aim of this scheme is to generate tunable, intense THz radiation.

Fig. 2 shows the electron beam behavior as it moves through the modulator and chicane sections. The theoretical explanation of density modulation of the relativistic electron beam is given in Ref. [27] in a more detail way. In Fig. 2, we present the numerical solution of uniformly distributed electron beam at the entrance of the first modulator. The dimensionless energy parameter p, as a function of longitudinal coordinate z normalized by first laser wavelength has been shown. Fig. 2 shows that the longitudinal phase space is periodic with period length $10\lambda_1$. The laser spikes are printed on the electron beam longitudinal phase space profile p. The magnitude of energy modulation is enhanced in the second modulator (Fig. 2(b)). Here the electron beam is energy modulated by the second laser with different wavelength. After chicane section as shown in Fig. 2(c), the longitudinal phase space gets smeared by the chicane with finite momentum compaction factor R_{56}.

In the next section, simulation results are presented for the density modulation of the relativistic electron beam and the THz radiation generation. To track the beam dynamics we use six dimensional phase space tracking code ELEGANT [29].

3. Simulation results for tunable THz radiation generation

For simulation, the selection of electron beam parameters is chosen from the existing fs–THz beamline at PAL [25]. A moderately relativistic 70 MeV electron beam accelerated on-crest in the linac is considered. The used wavelengths of the external lasers are equivalent to 800 nm which is fixed and second laser's variable wavelength. The length of the first modulator is chosen $5\lambda_{w1}$ with wiggler period λ_{w1} equal to 3.2 cm. The length of second modulator is chosen $5\lambda_{w2}$with wiggler period λ_{w2} equal to 2.2 cm. Both laser's beam spot sizes are chosen $\omega_0 = 400$ μm and pulse duration is 2 ps full-width half maximum (FWHM). The electron bunch size is taken 500 μm and the length of the electron bunch is around 6 ps. Modulators are resonated at their respective laser frequency.

The FEL resonance condition is defined by $\lambda_L = \lambda_u/2\gamma^2(1 + K_w^2/2)$ where $K_w = eB_0/mck_w$ is the undulator parameter, λ_L is the laser wavelength, $k_w = 2\pi/\lambda_u$ is the wiggler wave vector, and λ_u is the undulator period. The relativistic γ factor is 137 corresponding to 70 MeV electron beam energy.

It was estimated that 200,000 particles are enough to get the accurate result in the beam transport simulation. The space charge effects are considered in the calculations. As earlier mentioned, this scheme is based on the down conversion of the frequency. After dispersion section, different frequencies of density modulations are obtained according to the following relation:

$$k_{n,m} = (nk_1 - mk_2) \quad (1)$$

where n and m are integer numbers and k_1 and k_2 are the wave numbers of first and second laser. The second laser can be generated from the optical parametric amplifier (OPA) technique. The OPA pumped by Ti:sapphire laser at 800 nm can easily provide a tunable signal [30]. The summary of simulation parameters is given in Table 1.

3.1. Electron beam density modulation and the THz radiation generation

Fig. 3(a) shows the current modulation spectrum of the electron beam chosen after chicane section. The laser wavelength for the first laser-modulator system is taken as 800 nm and for second laser-modulator system as 1550 nm. Both laser's pulse durations are 2 ps in FWHM. If we look at the current profile, in the absence of second laser, we do not see any current modulation (black line). The related RMS energy spread of electron beam was found to be 16 keV. For finite value of second laser power, we see

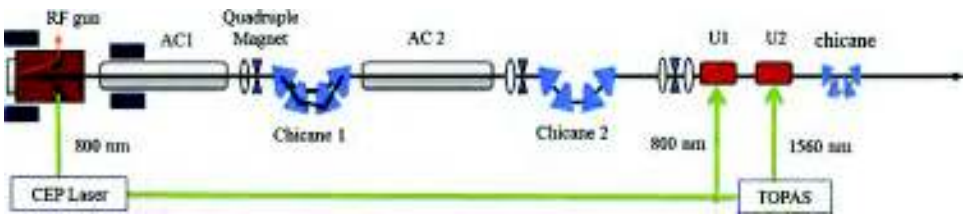

Fig. 1. Proposed fs–THz facility at PAL for 10 THz radiation generation.

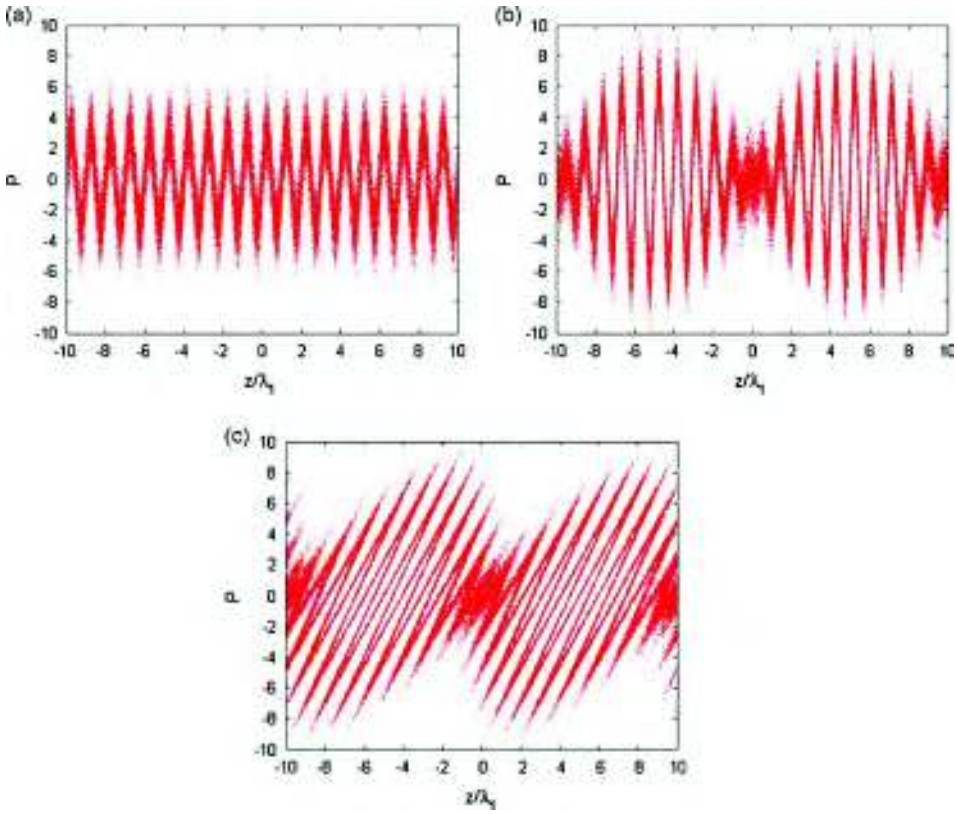

Fig. 2. Behavior of the longitudinal phase space distribution of electron beam, (a) after first modulator, (b) after second modulator and (c) after a dispersion section with finite R_{56}.

Table 1
Simulation parameters for the density modulated THz source at PAL.

Beam energy, E	70 MeV
Beam charge	0.2 nC
Slice energy spread	9.8 keV
Electron beam size	500 μm
RMS energy spread	24 keV
Average peak current	40 A
First laser wavelength in U1	800 nm
Second laser wavelength in U2	1550 nm
Lasers beam-waist size	400 μm
Undulator period length for U1	2.2 cm
Undulator period length for U2	3.2 cm
Number of periods for U1 and U2	5
Momentum compaction factor R_{56}	0.386 mm

the current modulation. For $P_{L1}=20$ MW, we find significant current modulation (blue line). Here the rms energy spread turns out to be 24 keV. For higher laser power 200 MW, we notice enhanced current modulation with large amplitude oscillatory peaks (red line). Corresponding RMS energy spread in this case reaches up to 55 keV. Both lasers induce the energy spread in the electron bunch longitudinal energy distribution. It is larger for large laser power. An electron bunch with such a large energy spread is sent to the chicane where density modulation takes place producing an increment in the magnitude of current peaks. Fig. 3 (b) and (c) shows the longitudinal energy distribution profile ($\Delta E/E$) as a function of electron bunch length. These profiles are chosen after second modulator section. For maximum energy modulation proper overlapping between laser and electron beam is considered. In simulation, the electron beam size is chosen as 500 μm and laser beam size is 400 μm good enough for maximum interaction. Fig. 3(b) shows the longitudinal energy distribution for $P_{L2}=200$ MW. Fig. 3(c) shows the longitudinal energy distribution for $P_{L2}=20$ MW. From Fig. 3(b) and (c), it is clear that induced energy spread in the central part is larger for $P_{L2}=200$ MW compared to $P_{L2}=20$ MW.

To obtain the radiation in frequency domain, the frequency Fourier transform (FFT) of the time domain spectrum of current modulation is taken. Fig. 4(a) shows the electron beam current modulation spectrum taken after chicane. Here the lasers wavelengths are 800 nm and 1550 nm and lasers power is 200 MW. The length of the electron bunch is 6 ps and the laser pulse duration is 2 ps FWHM. Fig. 4(b) shows the FFT of the current modulation shown in Fig. 4(a). In Fig. 4(a), the laser spikes are clearly printed in the current profile. Fig. 4(b) gives 12 THz frequency as the dominant frequency obtained by FFT of the current modulation spectrum. This is confirmed by Eq. (1) for $n=1$ and $m=-2$ and for laser wavelengths 800 nm and 1550 nm. To obtain this frequency, we did electrons slice (fractional part of the electron beam) optimization to reduce the numerical noises in the simulation. It was found that 200 number of analysis slices appeared a good number for 12 THz. The selection of number of analysis slices is vital otherwise the possibility of side-bands of this frequency may appear due to numerical noises present in the FFT spectrum. One can see that the energy modulation of electron bunch takes place only in the central part of the electron bunch. In Fig. 4(b), there is a secondary peak at 22 THz which is supposed to be an image frequency of 12 THz.

To further enhance the amplitude of the THz radiation as shown in Fig. 4(b), we study the effect of second laser power and its beam-waist size on the amplitude of the THz radiation. We keep all the parameters the same as considered in Fig. 4.

3.2. *Effect of laser parameters on the amplitude of the THz radiation*

For greater amplitude of the THz radiation, in Fig. 5(a), we calculate the amplitude as a function of second laser power. One can notice from Fig. 5(a), the amplitude increases linearly with the

laser power. The beam-waist size of both lasers is 400 μm. The modulators are tuned at laser frequencies 800 nm and 1550 nm. In Fig. 5(b), the THz amplitude is simulated as a function of laser beam-waist size. This time the laser powers are kept fixed at 20 MW. It was found that the amplitude increases linearly with the laser beam-waist size. One can see, after $\omega_0 = 360$ μm, the amplitude of the THz radiation becomes almost constant up to $\omega_0 = 520$ μm. Here the electron beam size is 500 μm.

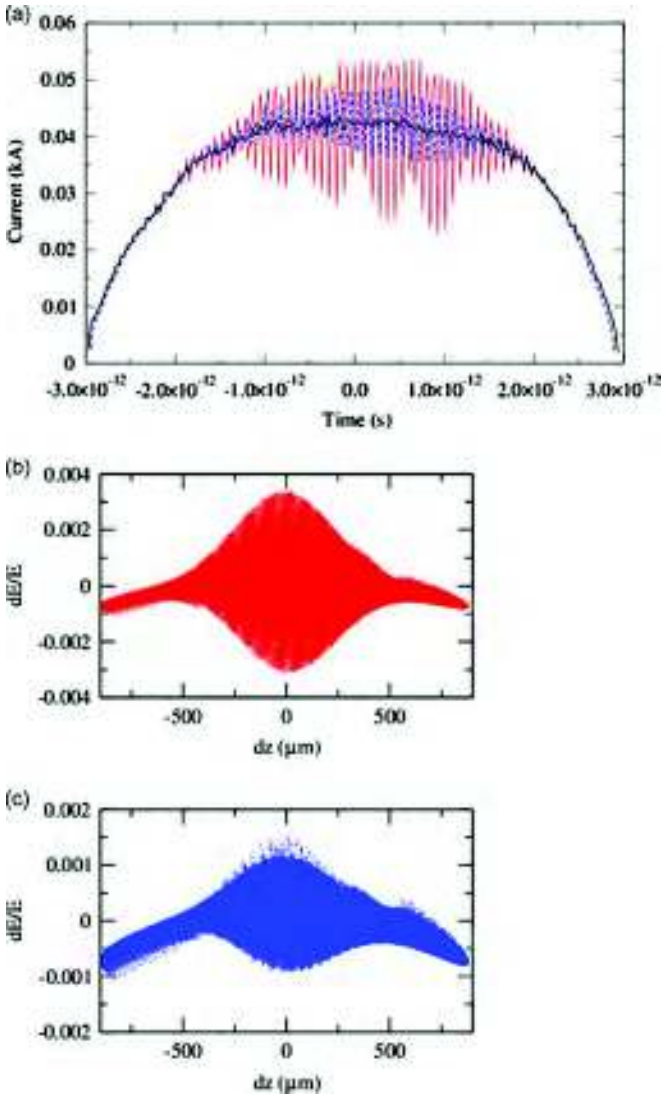

Fig. 3. (a) Black line indicates the current modulation of electron beam without second laser, $P_{L2} = 0$ MW, red line for $P_{L2} = 200$ MW, and blue line for $P_{L2} = 20$ MW. The longitudinal energy distribution of electron beam taken after second modulator, (b) for $P_{L2} = 200$ MW, and (c) for $P_{L2} = 20$ MW. The first laser power is $P_{L1} = 200$ MW. (For interpretation of the references to color in this figure legend, the reader is referred to the web version of this article.)

3.3. Effect of momentum compaction factor R_{56} on the amplitude of the THz radiation

Chicane is used to convert the energy modulation of electron bunch to the density modulation by making spatial rearrangement of the electrons. A chicane is made up of four dipole magnets. The distance between the first and the second dipole magnet and the distance between the third and the fourth dipole magnet are equal. A chicane deflects the electron trajectory of incoming electrons. Higher energy electrons cover the shorter path and lower energy electrons cover the longer path creating the density modulation of electrons. Corresponding momentum compaction factor (R_{56}) is optimized for maximum THz radiation amplitude. R_{56} depends on the bending angle θ_B of the dipole magnet and the length L_1 between first two and last two dipole magnets and L_B is the effective length of dipole in chicane: $R_{56} \approx -2\theta_B^2(L_1 + 2/3L_B)$. Here, bending angle θ_B and length L_1 are the free parameters. We prefer a small bending angle for emittance dilution and to avoid the coherent synchrotron radiation inside the dipole magnets. The length between the dipoles is minimized so that the length of the whole system is as small as possible.

To improve amplitude characteristic of THz radiation further, we optimize the R_{56} parameter as shown in Fig. 6. In this regard, we change the bending angle θ_B to enhance the THz radiation amplitude. We notice that it increases linearly up to certain R_{56} and then it starts to decrease. The maximum amplitude corresponds to $R_{56} = 0.386$ mm; for $L_1 = 0.07$ m and bending angle $= 2.4^\circ$.

3.4. Tunable THz radiation generation

In this section, the effect of second laser wavelength has been studied on the THz radiation frequency. Combination of a Ti sapphire laser with an OPA scheme can allow one to generate tunable THz radiation covering a wide frequency range using laser-modulated electron beams. To make it tunable, we vary the second laser wavelength. In Fig. 7, we present few sets of simulation results showing tunable THz radiation frequency. The depth of the modulation and the modulation period directly depend on the laser wavelength. By varying the second laser wavelength, we simulated different THz radiation frequencies. First laser wavelength is kept fixed at 800 nm and second laser wavelength is varied from 1520 nm to 1570 nm. In Fig. 7, the resultant radiation frequency is shown as a function of second laser wavelength. The

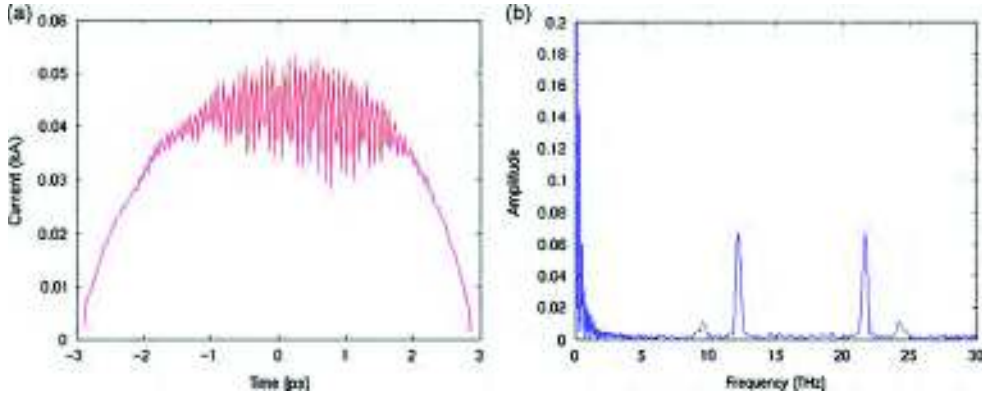

Fig. 4. (a) The current modulation of the electron bunch taken after chicane and (b) corresponding FFT spectrum.

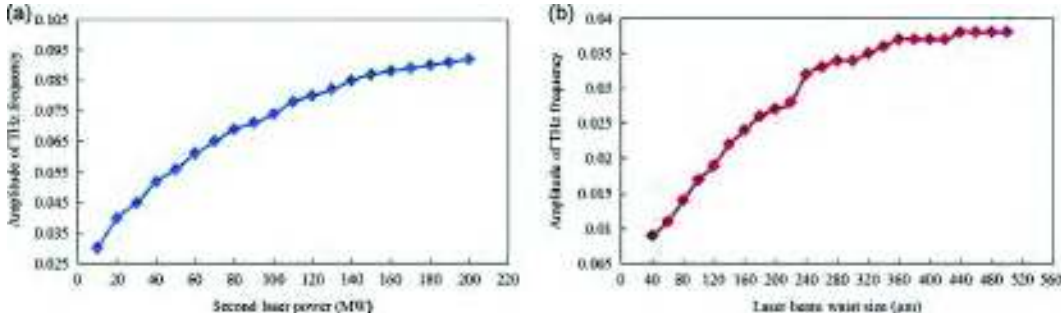

Fig. 5. (a) The amplitude of the THz radiation as a function of second laser power, and (b) the amplitude of the THz radiation as a function of second laser beam-waist sizeω_0. Other parameters are the same as in Fig. 4.

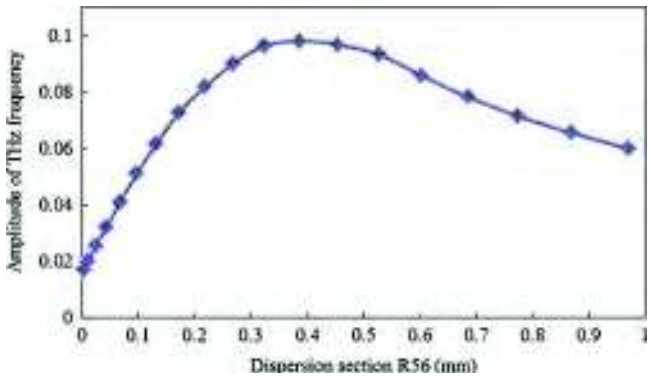

Fig. 6. The amplitude of the THz radiation as a function of R_{56} (by varying bending angle θ_B). Other parameters are the same as in Fig. 4.

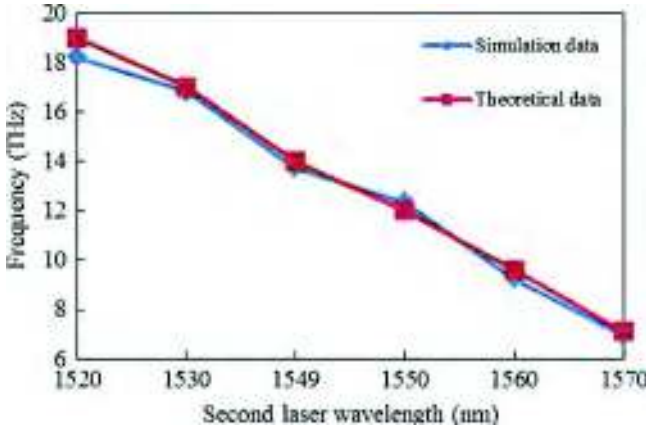

Fig. 7. Tunable THz radiation generation as a function of second laser wavelength. Other parameters are the same as in Fig. 4.

theoretical data is obtained by Eq. (1) for $n=1$ and $m=-2$. We find simulation results and the theoretical data are in close proximity.

The number of analysis slices varies from 200 to 300 corresponding to second laser wavelength 1520–1570 nm. The presence of space charge force in gun and accelerator part does not affect the resultant THz radiation frequency and its amplitude. To realize this scheme at PAL, a further study would be to analyze the echo effect [20,21] on the density modulated THz radiation frequency. For this analysis, one more chicane would be introduced between first and second modulator section. The effect of this chicane and the effect of chirped electron beam would be separately studied on the central frequency of the density modulated electron beam.

3.5. The extraction scheme for the THz radiation

To extract THz radiation generated by a relativistic electron beam, coherent transition radiation (CTR) and coherent synchrotron radiation (CSR) using bending magnets are widely used. At the fs–THz facility, we use the CTR method to measure the THz radiation. The transition radiation from the electrons becomes coherent at wavelengths that exceed the longitudinal length of the electron bunch. Hence, intense fs–THz pulses with pulse duration comparable to the electron bunch length can be generated by the CTR method [12–14]. Here, the total electron bunch length is 6 ps approximately, and the effective density modulation is only in the central part of the electron bunch. Hence, the entire electron bunch will not contribute to the CTR. Only the density modulated part of the electron bunch will offer to the CTR. At the fs–THz facility, the CTR target is a 1 in. diameter Al foil with a thickness of 1 μm (or Cu mirror), and the diameter of the electron beam is 500 μm at the target. The radiated THz pulses are extracted from the LINAC vacuum pipe through a wedged chemical vapor deposition (CVD) diamond window (diameter 24 mm, central thickness 0.7 ± 0.1 mm, wedge angle $0.5\pm0.1^\circ$, Diamond Materials GmbH) [25].

4. Conclusion

We presented an analysis of terahertz radiation from the relativistic density modulated electron beam. For maximum density modulations, both lasers need to interact with the electron beam simultaneously which requires the lasers to overlap with the electron beam both spatially and temporally in both modulators. Since the laser pulse is shorter than the electron bunch length, density modulation is only present in the central part of the bunch.

Using the fs–THz beamline parameters at PAL, we have shown in our simulation that with 800 nm and 1550 nm lasers combination we can generate 12 THz radiation frequency by down conversion of the laser frequency. We found that laser power, laser beam waist-size; and chicane parameter R_{56} play an important role to further improve the amplitude of the THz radiation. Our study shows that for other laser wavelength combinations also, tunable, synchronized THz radiation can be generated. In our simulation, the selection of electron slices number becomes important for different laser wavelength combinations to obtain tunable THz radiation. The proper synchronization of this radiation to the laser will enable high temporal resolution in the pump–probe THz experiment. This intense narrowband THz source will

facilitate the study of the samples which come under the THz regime.

Acknowledgments

This research was supported partially by Basic Science Research Program through the National Research Foundation (NRF) funded by the Ministry of Education, Science and Technology (Grant no. 2010-0012016), by the Nuclear Research Foundation of Korea grant funded by the Korea government (MEST) (No. 2012027506), by MSCP and PAL, Korea.

References

[1] G.P. Williams, Report on Progress in Physics 69 (2006) 301.
[2] K. Reimann, Report on Progress in Physics 70 (2007) 1597.
[3] M. Tonouchi, Nature Photonics 1 (2007) 97.
[4] G.R. Neil, et al., Nuclear Instruments and Methods in Physics Research A 507 (2003) 537.
[5] M. Wulff, et al., Nuclear Instruments and Methods in Physics Research A 398 (1997) 69.
[6] J. Yang, et al., Nuclear Instruments and Methods in Physics Research A 629 (2011) 6.
[7] P. Emma, Nature Photonics 4 (2010) 641.
[8] H. Tanaka, et al., Nature Photonics 6 (2012) 540.
[9] T. Ikeda, et al., Applied Physics Letters 87 (2005) 034105.
[10] G.L. Carr, et al., Nature 420 (2002) 153.
[11] J.M. Byrd, et al., Physical Review Letters 89 (2002) 224801.
[12] W.P. Leemans, et al., Physical Review Letters 91 (2003) 074802.
[13] Y. Shen, et al., Physical Review Letters 99 (2007) 043901.
[14] S. Casalbuoni, et al., Physical Review Special Topics: Accelerators and Beams 12 (2009) 030705.
[15] S. Bielawski, et al., Nature Physics 4 (2008) 390.
[16] J. Neumann, et al., Journal of Applied Physics 105 (2009) 053304.
[17] L.H. Yu, Physical Review A 44 (1991) 5178.
[18] L.H. Yu, et al., Science 289 (2000) 932.
[19] G. Lambert, et al., Nature Physics 4 (2008) 296.
[20] G. Stupakov, Physical Review Letters 102 (2009) 074801.
[21] D. Xiang, G. Stupakov, Physical Review Special Topics: Accelerators and Beams 12 (2009) 030702.
[22] Y. Ding, Z. Huang, R.D. Ruth, Physical Review Special Topics: Accelerators and Beams 13 (2011) 060703.
[23] E. Allaria, et al., Nature Photonics 6 (2012) 699.
[24] J. Yan, et al., Nuclear Instruments and Methods in Physics Research A 621 (2010) 97.
[25] J. Park, et al., Review of Scientific Instruments 82 (2011) 013305.
[26] R.W. Boyd, Nonlinear Optics, 2nd edition, Academic Press, New York, 2003.
[27] D. Xiang, G. Stupakov, Physical Review Special Topics: Accelerators and Beams 12 (2009) 080701.
[28] M. Dunning, et al., Physical Review Letters 109 (2012) 074801.
[29] M. Borland, Proceedings of the 6th International Computational Accelerator Physics Conference, Darmstadt, Germany, September 2000.
[30] G. Cerullo, S. De Silverstn, Review of Scientific Instruments 74 (2003) 1.